Green Chemistry

Accepted Manuscript

ROYAL SOCIETY OF CHEMISTRY

www.rsc.org/greenchem

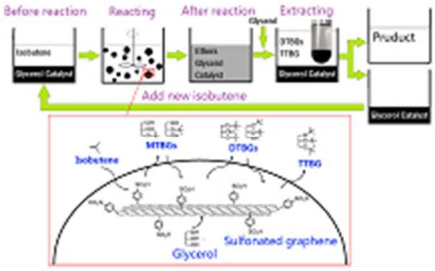

61x38mm (96 x 96 DPI)

Sulfonated graphene catalyzes the etherification of glycerol and isobutene with high multi-ethers yield and little deactivation in repeat uses.

Cite this: DOI: 10.1039/c0xx00000x

www.rsc.org/xxxxxx

ARTICLE TYPE

Etherification of glycerol with isobutene on sulfonated graphene: reaction and separation

Jinxia Zhou*[a], Yu Wang[a], Xinwen Guo[b], Jingbo Mao[a], Shuguang Zhang*[a, b]

Received (in XXX, XXX) Xth XXXXXXXXX 20XX, Accepted Xth XXXXXXXXX 20XX

DOI: 10.1039/b000000x

Sulfonated graphene catalyst (SG) prepared by grafting sulfonic acid-containing aryl radicals to the two-dimensional surface of graphene was used for the etherification of glycerol with isobutene, and a reaction-extraction process was developed for easy realization of product isolation and catalyst recycle. With its ultra thin two-dimensional open substrate, stable sulfonic acid sites, amphiphilic property and light texture, SG exhibited excellent catalytic performance in the etherification reaction. At 60-70 °C with 4 wt% catalyst loading and a molar ratio of isobutene/glycerol 4, nearly a complete conversion of glycerol in 7 h and a selectivity of more than 90 mol% to desired multi-butyl glycerol ethers were achieved. Moreover, undesired oligomerization of isobutene was successfully suppressed. When extracted with fresh glycerol, the mixture after reaction was successfully layered to two phases, with a transparent liquid containing no less than 96 wt% di- and tri- butyl glycerol ethers in the top phase as product and a black mixture consisting of glycerol and SG in the bottom phase which can be used to start a new run with fresh isobutene addition. During six consecutive reaction-extraction cycles the catalyst maintained its robust performance.

1 Introduction

The diminishing availability of petrochemical resources and the increasing environmental problems boost the production and use of sustainable resources.[1] Glycerol, a renewable compound, which has been traditionally produced as a byproduct from the steam splitting or saponification processes of animal fat and vegetable oil, now is also available as a major byproduct of biodiesel production processes in the amount of approximately 10 wt% of the feedstock.[2,3] Moreover, glycerol production through biological fermentation process based on the cheap and abundant materials, cellulolytic derivatives, is booming quickly, and will be another access to the production of glycerol.[4,5,6,7] With the increasing glycerol production, great interest has been addressed to the development of new routes for versatile uses of glycerol. Among various possibilities, one promising option is the catalytic etherification of glycerol with isobutene or tert-butanol to form mono-butyl glycerol ethers (MTBGs: 3-tert-butoxy-1,2-propanediol and 2-tert-butoxy-1,3-propanediol), di-butyl glycerol ethers (DTBGs: 2,3-di-tert-butoxy-1-propanol and 1,3-di-tert-butoxy-2-propanol), and tri-butyl glycerol ethers (TTBG: 1,2,3-tri-tert-butoxy pro-pane, TTBG).[8,9]

DTBGs and TTBG, the so-called "multi-butyl glycerol ethers", can be used as additives for diesel and biodiesel reformulation, which improve the low temperature properties of diesel fuel (pour point and cold filter plugging point) and reduce the viscosity of biodiesel fuel.[10] On the contrary, MTBGs are not suitable to be used as diesel additive because their solubility in diesel is low.[11] Therefore, the etherification of glycerol must be directed to maximize the yield of DTBGs and TTBG.[8] As for the tert-butylation reagent, both isobutene and *tert*-butanol are widely used, and the etherification using isobutene is prone to yield higher conversion and selectivity to multi-butyl glycerol ethers than the etherification using tert-butanol.[1] The use of isobutene is favoured also because of the easy separation of residual isobutene after the reaction from the liquid phase products with a flash unit. A disadvantageous aspect of using isobutene as the alkylation agent is that the formation of di-isobutenes (DiB, mixture of 2,4,4-trimethyl-1-pentene and 2,4,4-trimethyl-2-pentene,) via oligomerization is normally inevitable.[12] This oligomerization results in an undesired consumption of isobutene and DiB also is problematic when formulated with fuels.[13, 14] Therefore, the effort of etherification of glycerol with isobutene should be focused on improving the selectivities to diethers and triether and at the same time minimizing isobutene oligomerization.

To date, many catalysts, including homogeneous acid catalysts such as *p*-toluenesulfonic acid,[15,16] phosphorustungstic acid,[16]

[a]*College of Environmental and Chemical Engineering, Dalian University, Dalian, 116012, China.*

[b]*State Key Laboratory of Fine Chemicals, Dalian University of Technology, Dalian, China.*

Email: zhoujxmail@163.com (J. Zhou), rich_s_zhang@yahoo.com (S. Zhang).

Fax: +86 411 87402449; Tel.: +86 411 87403214.

ionic liquids,[15,17] and heterogeneous catalysts like acidic resins,[16,18-22] zeolites,[19,23-25] acid-functionalized mesostructured silicas,[13] sulfonated carbon catalysts[26,27] have been studied for the etherification of glycerol with isobutene. Table 1 lists some representative results from recent publications. Hee Jong Lee et al[15] compared the catalytic performances of three kinds of homogeneous catalysts, silicotungstic acid, an ionic liquid containing sulfonic acid groups and *p*-toluenesulfonic acid. Silicotungstic acid has strong acidity and tends to promote isobutene oligomerization; the ionic liquid has good solubility in glycerol and MTBGs but poor solubility in multi-butyl glycerol ethers, so it demonstrates the feature of suppressing TTBG formation; *p*-toluenesulfonic acid has lower acid strength compared to silicotungstic acid, but it shows the best performance among the three. Not only is the selectivity towards DTBGs and TTBG the highest (total 88 mol%), but also the selectivity to DiB is negligible in *p*-toluenesulfonic acid-driven reaction. However, *p*-toluenesulfonic acid is more difficult to be recycled, and traces of the acid that could not be extracted from the product mixture deteriorates the yields of ethers during the downstream distillation step.[9] Although *p*-toluenesulfonic acid is not the best-fit catalyst for this reaction, it offers certain enlightenment that the acid sites derived from sulfonic acid groups are promising for catalyzing this reaction.

In recent years, a series of heterogeneous catalysts containing sulfonic acid groups have drawn great attentions. Acid-based resins like Amberlyst 15 and Amberlyst 35, whose functional groups are the analogue of *p*-toluenesulfonic acid, have shown superior glycerol conversion as well as desirable selectivity to multi-butyl glycerol ethers, but they promote high degree of isobutene oligomerization, producing up to 36.2 wt% DiB in the product.[16,18-22, 28] González et al[29] used sulfonated zeolites like Beta and ZSM-5 as catalysts for this reaction and found that due to the incorporation of the sulfonic groups, all the modified zeolites showed improved catalytic performances. But these catalysts deactivates progressively during consecutive catalytic runs, and the oligomerization of isobutene still is not negligible (up to 10 wt%). The catalytic performances of spherical silica supported Hyflon catalysts[30] and sulfonated peanut shell catalyst[27] are similar to those of sulfonated zeolites, except that the DiB formation is a little lower (less than 5 wt%). Recently reported sulfonated aerogel is a rare solid catalyst that could effectively suppress DiB formation, probably due to its readily accessible structure.[28]

Table 1 Representative results of glycerol etherification with isobutene from recent publications [a].

Entry	Catalyst	Reaction condition	Conv.$_{Gly}$ (%)	Selectivity (mol%)			DiB (wt%)	Ref.
				MTBGs	DTBGs	TTBG		
1	*p*-toluenesulfonic acid (PTSA)	$R_{IB/Gly}$, 4; $R_{cat/Gly}$, 7.5 wt%; 60 °C; 5 h	100	18	60	22	0.2	15
2	Silicotungstic acid ($H_4SiW_{12}O_{40}$)		93	35	58	7	17	
3	Sulfonated ionic liquid		85	51	43	6	0.5	
4	Amberlyst 15 powder		100	16	60	24	22	
5	Sulfonated peanut shell catalyst	$R_{IB/Gly}$, 4; $R_{cat/Gly}$, 6 wt%; 70 °C; 2 h	100	7.9	60.0	32.1	2.5	27
6	Sulfonated silica aerogel	$R_{IB/Gly}$, 4; $R_{cat/Gly}$, 5 wt%; 75 °C; 24 h; N_2, 10 bar	99	25	58	17	-	28
7	Amberlyst-15		99	23	56	19	36.2	
8	Sulfonated Beta	$R_{IB/Gly}$, 4; $R_{cat/Gly}$, 5 wt%; 75 °C; 24 h; N_2, 10 bar	100	9	55	36	9.4	29
9	Sulfonated ZSM-5		100	16	56	28	3.9	
10	Hyflon supported on spherical silica	$R_{IB/Gly}$, 4; $R_{cat/Gly}$, 7.5 wt%; 70 °C; 6 h	100	2.6	46.7	50.7	4.5	30

[a] Some results were deduced from the figures listed in the publications.

The different performances of these sulfonic acid-functionalized catalysts are partially attributed to the characteristics of the base materials that are used for grafting the sulfonated groups. This guides us adopting a novel substrate material, graphene, to craft the sulfonated catalysts for the etherification of glycerol with isobutene. Graphene, which consists of two-dimensional carbon sheets with one-atomic thickness, has great potential in various applications due to its unique physical and chemical properties.[31] Pristine graphene is composed of sp^2-hybridized carbon atoms arranged in a honeycomb lattice of a planar layer. At present, graphene can be largely prepared from the reduction of graphene oxide (GO), an intermediate which is typically obtained from the treatment of natural sources of flake graphite under strong acidic and oxidizing conditions.[32,33] Synthetic graphene tends to contain certain lattice defects both on its surface and around its periphery.[34] Some sp^3-hybridized carbon atoms anchor certain amount of suspended hydrogen bonds, which have capabilities of reacting with other organic functional groups.[35] Functionalized graphene materials are amphiphilic with hydrophilic groups on a more hydrophobic basal plane, which can act like surfactant, as measured by their ability to disperse on interfaces.[36] Combining its excellent mechanical properties, large surface area, distinctive two-dimensional structure and accessible active sites to graft a decent amount of functional groups, graphene provides an ideal platform for the formation of novel heterogeneous catalysts.[37-40]

In the present work, sulfonated graphene catalyst was synthesized through grafting functional groups similar to *p*-toluenesulfonic acid onto the two-dimensional surface of graphene and was tested for the etherification of glycerol with isobutene. Characterizations with various tools were carried out aiming to correlate the catalyst's physical and chemical properties with its catalytic performance. Special attention was paid to develop a simple but efficient method for product isolation as well as catalyst recycle.

2. Experimental

2.1 Catalyst preparation

GO was prepared following a modified Hummers' method which was originally presented by Kovtyukhova and colleagues.[33] Briefly, graphite (SP, Sinopharm Chemical Reagent Co., Ltd.,

China) was pre-oxidized with concentrated H_2SO_4 (96-98%, Comio Chemical Reagent Co., Ltd., China), $K_2S_2O_8$ (>99%, Sinopharm Chemical Reagent Co., Ltd., China), and P_2O_5 (>99%, Aladdin, China). Then it was further oxidized with concentrated H_2SO_4 and $KMnO_4$ (>99.5%, Comio Chemical Reagent Co., Ltd., China). The reaction was terminated by the addition of deionized water and 30% H_2O_2 solution (30% in water, Comio Chemical Reagent Co., Ltd., China). The as-synthesized graphite oxide was washed with 1 M HCl aqueous solution (37%, Dandong Chemical Reagent Co., Ltd., China) and deionized water through repeated dispersions and centrifugations in order to remove metal ions and acids. Finally, it was subjected to dialysis for a week to completely remove residual salts and acids. GO was generated when 0.5 wt% graphite oxide was dispersed in water with ultrasonic vibration. The obtained brownish solution was left undisturbed for 24 h so that any unexfoliated graphite oxide (very small amount) would settle down and be separated by decantation. The obtained GO suspension (2000 mL, 1.0 $mg \cdot mL^{-1}$) was reduced with 20 mL 80% hydrazine hydrate (80% in water, Sinopharm Chemical Reagent Co., Ltd., China) at 95 ^oC for 24 h followed by filtering and washing with 2 L deionized water. The yielded filter cake was dried with freeze-drying method to get a purified reduced graphene oxide (RGO).

4-Benzenediazoniumsulfonate was synthesized by the diazotization of sulfanilic acid. With continuous stirring, sulfanilic acid (>99.8%, Sinopharm Chemical Reagent Co., Ltd., China) was dispersed in 1 M HCl aqueous solution in a flask placed in an ice water bath at 1-3 ^oC; 1 M $NaNO_2$ (>99%, Sinopharm Chemical Reagent Co., Ltd., China) aqueous solution was added into the flask dropwise and a clear solution was obtained after all the $NaNO_2$ was in. The molar ratio of sulfanilic acid:$NaNO_2$:HCl was 10:11:100. After stirring for another hour at the temperature, a white precipitate formed. It was filtered and washed thoroughly with cool deionized water. The filter cake was sealed and kept at 1-3 ^oC in a refrigerator. Due to its instability in dry form, the 4-Benzenediazoniumsulfonate synthesized with the procedure above was used without heat treatment after the washing and vacuum filtration.

A typical RGO sulfonation process was as follows: a three-neck round flask with a certain amount of ethanol (>99.7%, Comio Chemical Reagent Co., Ltd., China) was placed in an ice water bath controlled at 3-5 ^oC, RGO was dispersed in the ethanol under ultrasonic vibration, and then with continuous stirring 4-Benzenediazoniumsulfonate was transferred into the flask, subsequently half dosage of 50 wt% H_3PO_2 aqueous solution (50 wt% in water, Wuhan Jiangrun Fine Chemical Co., Ltd.) was added. After stirring for 40 min, another half dosage of H_3PO_2 solution was added and the stirring was continued for 1 h. The dosage ratio of ethanol (ml) : RGO (mg) : 4-Benzenediazoniumsulfonate (g) : 50 wt% H_3PO_2 (ml) was 36 : 75 : 1 : 72. The obtained sulfonated graphene was filtered, washed with 1 M HCl (100 mL) and deionized water. The final filter cake was further purified by freeze drying. The treated sample was labeled as SG.

2.2 Catalyst characterization

X-ray powder diffraction (XRD) patterns were recorded at room temperature on a Rigaku Miniflex (M/s. Rigaku Corporation, Japan) X-ray diffractometer using Ni filtered Cu Kα radiation (λ = 1.5406 Å) with a scan speed of 1 ^{o}/min and a scan range of 2-80^o at 30 kV and 15 mA. The contents of carbon, hydrogen, oxygen and sulfur in graphene-based catalysts were obtained with Elemental Analyzer vario EL cube for simultaneous CHNS analysis with options for O analysis. Characterizations with transmission electron microscopy (TEM) were carried out on a JEOL JEM-2011TEM. To prepare samples for the TEM study, graphene derived samples were dispersed in water, and deposited onto copper grids. Scanning electron images (SEM) were taken on a QUANTA 200FEG microscope. Thermogravimetric analysis (TGA) results were acquired on a TGA/SDTA851e instrument (Mettler Toledo). Samples were heated in a flow of N_2 gas (20 mL/min) from room temperature to 700 ^oC with a ramp rate of 10 ^oC /min. Surface area measurement with nitrogen adsorption was performed with a Micromeritics ASAP 2020. Raman spectroscopy was performed using a Renishaw InVia Raman microscope with a solid-state laser (excitation at 532 nm, 0.3 MW and 600 s). The graphene's thickness was structurally characterized with atomic force microscopy (AFM) using a Nanoscope III equipped with 1553D scanner (Digital Instruments Inc., Santa Barbara).

2.3 Catalytic performance measurement

Glycerol (>99%, China National Medicines Corporation Ltd., China) and isobutene (>99.5%, Dalian Airchem Specialty Gases and Chemicals Co., Ltd., China) were used as reactants. Etherification experiments were performed in oil bath heated stainless steel autoclaves (15 mL) equipped with feedstock line connectors and a pressure gauge. The temperature and stirring were controlled by IKA magnetic Stirrers (IKA-Werke GmbH & Co. KG - A company, Germany). The stirring rate was set at 1000 RPM to overcome external diffusion limitation. The composition of the feed mixture was 1 g of glycerol, Isobutene/Glycerol molar ratio ($R_{IB/Gly}$) from 3/1 to 6/1, and catalyst loading (wt% of glycerol, $R_{cat/Gly}$) from 1 wt% to 7 wt%. For a typical run, a specific amount of glycerol and dry catalyst were firstly loaded into the reactor. After the reactor was flushed with nitrogen to remove air, isobutene was injected into the reactor under 0.5 MPa of nitrogen pressure, and then the pressure in the reactor was adjusted to 1.0 MPa with nitrogen. The oil-bath was preheated to a given temperature, and the reaction time started to count as the autoclave was putted in it. Each reaction usually lasted for 7 h at the reaction temperature. After a specified reaction period, the reaction was quenched immediately with cool water. The pressure was slowly reduced to atmospheric pressure. Any unreacted isobutene would be vaporized and released together with N_2. To obtain clean liquid for composition analysis on gas chromatograph (GC), 10 μL of the liquid product and catalyst mixture was taken, diluted with ethanol and then filtered to remove the catalyst.

In the cases that involved collecting the products as well as recycling of the catalyst, an extraction step was applied to the reaction mixture obtained above. First, fresh glycerol in the amount same as the original loading (1 g) was added to the reactor. Then the mixture was stirred for 0.5 h at 800 RPM at room temperature. Finally the mixture was left undisturbed for

0.5 h for phase separation, forming a transparent liquid phase at the top phase and a black mixture phase containing catalyst at the bottom. The top liquid phase was taken out with a pipett and its mass was recorded. It contained no catalyst and the sample was analyzed with GC without filtration. The mass of the bottom phase was obtained by subtracting the mass of the bare reactor from the mass of the reactor with the bottom phase inside. This concluded the first reaction-extraction cycle. Fresh isobutene was charged to the reactor to start the next reaction cycle using the same catalyst. This cycle of reaction and extraction was repeated five more times to demonstrate the catalytic stability and the efficiency of the extraction. During the six consecutive reaction-extraction cycles which were affected by five samplings, the loss of catalyst would not be more than 2% and loss of liquid product would be within 0.4%.

GC analysis was conducted on a gas chromatograph (HP5890) equipped with a flame ionization detector. The column used was a PEG2W capillary column (30 m × 0.32 mm × 0.5 μm) manufactured by Dalian Institute of Chemical Physics, Chinese Academy of Sciences. Commercial compounds of glycerol, MTBGs (97%, from Aldrich) and 2,4,4-trimethyl-1-pentene (98%, from Aldrich, representative of di-isobutylene) were used as standard references to obtain corresponding response factors. The methods for establishing the response factors of DTGEs and TTGE and the calculation process of the glycerol conversion ($Conv._{Gly.}$) and the selectivities to MTBGs, DTBGs or TTBG have been described in our previous work.[23] For each sample, mass or mole percentages of glycerol, MTBGs, DTBGs, TTBGs and DiB were acquired according to the chromatogram areas and the response factors of these compounds. Data variation in this work is no more than ± 2% (relative value).

p-Toluenesulfonic acid (PTSA) (>99%, Sinopharm Chemical Reagent Co., Ltd., China) was tested for comparison purpose.

3 Results and discussion

3.1 Catalyst characterization

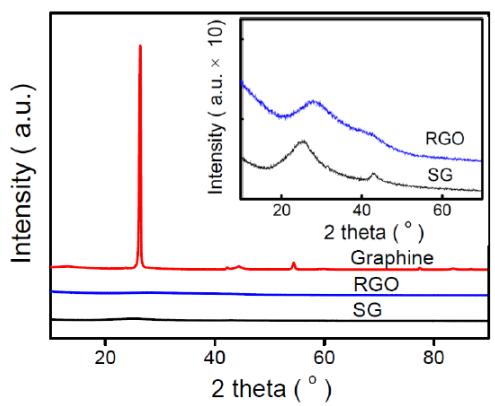

Fig. 1 XRD patterns of graphite, RGO and SG.

Fig.1 shows the XRD patterns of the starting material, graphite and its two derivatives, RGO and SG. The XRD pattern of graphite has a sharp peak at 2θ = 26.3°, a characteristic of the layered structure of highly crystallized graphite with a spacing distance 0.34 nm.[40] The much weaker intensity of this peak in the patterns of RGO and SG indicates a possibility of the destruction of the layered structure, which is further confirmed by tapping-mode AFM characterization (Fig. 2). The AFM image of drop-cast solution of SG in neutral water reveals that those small sheets dispersed on the mica surface have a thickness about 0.3 nm, which is in agreement with the reported thickness of graphene.[41]

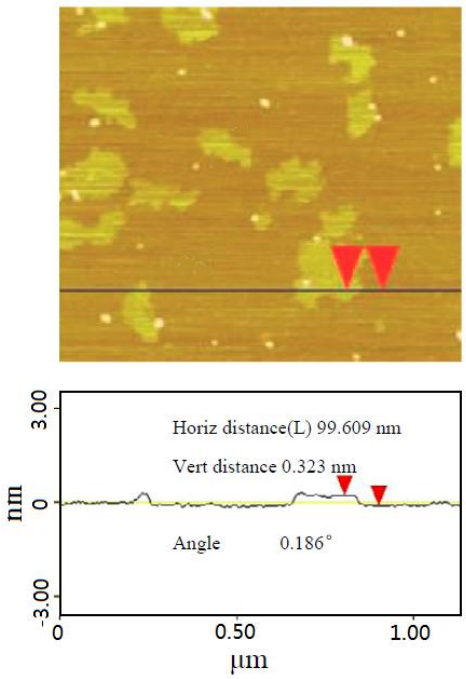

Fig. 2 AFM image of SG.

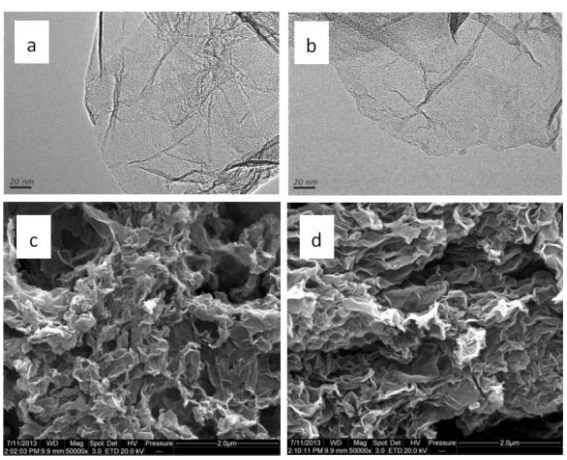

Fig. 3 TEM images of RGO (a) and SG (b); SEM images of RGO (c) and SG (d).

TEM images of RGO and SG in Fig. 3a and 3b show two-dimensional features with clear layers, which are similar to that reported by Jin et al.[42] Comparison of the two images discloses that the microstructure of the graphene sheets was intact during the sulfonation modification. It has been calculated that graphene has a large specific surface of 2630 m^2/g.[37] However, the BET

surface area of the RGO sample deduced from our nitrogen sorption isotherms is only 427 m^2/g. SEM images (Fig. 3c and 3d) reveals that the dried sheets of graphene and its derivatives pile up and shrink together. It is possible that some of the sheets might have overlaped and rallied closely, resulting in the BET value lower than the theoretical number. Once submerged in liquid, the graphene sheets will disperse like shown by the AFM image and exhibit a higher surface area.

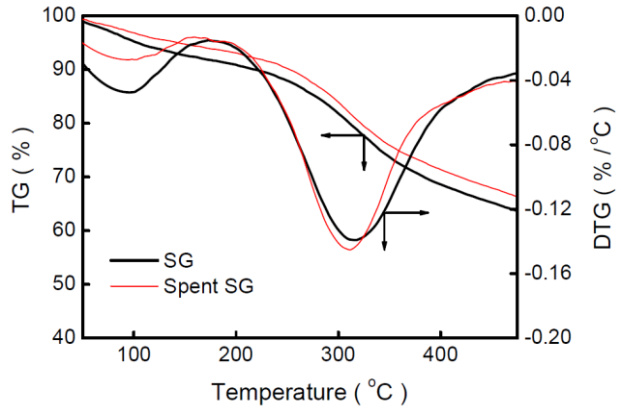

Fig. 4 TGA profiles of fresh SG and spent SG.

The TGA profiles of the fresh SG and the spent one are shown in Fig.4. SG is a derivative of RGO, and RGO is derived form GO. The TGA curve of GO (not shown in this paper) shows two sharp weight losses, one around 100 °C and the other between 180 and 230 °C, which are attributed to the evaporation of water and the decomposition of oxygen containing groups like hydroxyl, epoxy, carbonyl, and carboxyl groups, respectively. After the reduction, most of the oxygen containing groups on GO surface was removed, so the derived RGO had less weight loss. The weight loss in SG curve around 100 °C was the evaporation of moisture. The big difference of the TGA curves of RGO and SG started around 300 °C, above which SG's TGA pattern shows a sharp weight loss. Because SG is a derivative of RGO, we attribute this to the elimination of the carbon-carbon bonded benzenesulfonic-acid groups on SG because they are the components introduced to RGO through sulfonation. The weight loss behaviors of the fresh and spent catalysts above 200 °C are almost identical, which demonstrates the good thermal stability of the catalyst during the reaction.

Raman spectroscopes of the graphite, RGO and SG are shown in Fig. 5. Highly ordered graphite shows a strong Raman-active G band at 1585 cm^{-1} corresponding to the first-order scattering of the E2g mode for sp^2 carbon lattice and a weak disorder D band at approximately 1350 cm^{-1} resulted from the defects on the graphite edges.[43] Both the G and the D bands underwent significant changes in RGO and SG , manifesting that the original graphite's lattice was destroyed and the amount of the amorphous carbon increased in the graphite derivatives.[43] The strong defect-induced D bands in both RGO and SG Raman spectroscopies indicate that there is a certain fraction of sp^3 carbons among the sp^2 carbon network sheets of the two graphene materials, corresponding to sp^3 carbons with hydrogen groups in RGO and sp^3 carbons with benzenesulfonic acid groups in SG, respectively. Usually, a red or blue shift of a band can be used to evaluate the degree of structural change during chemical processing.[35] In our study, the G band shifted slightly from 1591 cm^{-1} in RGO to 1598 cm^{-1} in SG (blue shift), which is a qualitative indication of a successful introduction of the benzenesulfonic acid groups onto the sp^3 carbons in the sp^2 network. The exact amount of the groups is to be disclosed in the following discussion.

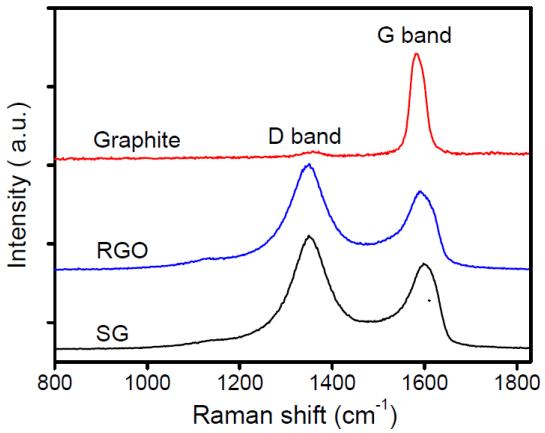

Fig. 5 Raman spectra of graphite, RGO and SG.

3.2 Catalytic performances of graphene based catalysts

3.2.1 Comparison of SG with PTSA and RGO

Table 2 Catalytic performances of SG, PTSA, and RGO for glycerol etherification with isobutene.[a]

Test#	Catalyst	$R_{IB/Gly.}$	Conv.$_{Gly.}$(%)	Selectivity (mol%)			DiB (wt%)
				MTBGs	DTBGs	TTBG	
1	SG	3:1	99.6	14.0	62.6	23.4	0.1
2	SG	4:1	99.7	7.9	56.4	35.7	0.3
3	SG	5:1	99.8	4.2	52.7	43.1	0.5
4	SG	6:1	99.5	2.8	38.6	58.6	0.6
5	PTSA[b]	4:1	93.5	45.2	49.2	5.6	0.1
6	RGO[c]	4:1	-	-	-	-	-
7	RGO+ PTSA[d]	4:1	94.5	40.3	51.8	7.9	0.1

[a] $R_{cat/Gly}$ = 4 wt%; 70 °C; 7h. [b] *p*-toluenesulfonic acid, PTSA= 13 mg; [c] RGO= 27 mg; [d] RGO= 27 mg; PTSA= 13 mg; "-", not detected.

Table 2 shows the reaction results of glycerol etherification with isobutene catalyzed by SG, PTSA and RGO as well as a mixture of RGO and PTSA. The glycerol conversions in the reactions catalyzed by SG were all close to 100%, and the total selectivity to DTBGs and TTBG was in the range of 86.0 mol% to 97.2 mol%. These values are similar to the best one in Table 1. SG catalyst consists of RGO as the substrate and benzenesulfonic acid groups as the active components. According to CHNSO elemental analysis, the sulfonate density on the SG catalyst was 1.9 mmol $(-SO_3H)\cdot g^{-1}$. This means that 40 mg SG catalyst ($R_{cat/Gly}$ = 4 wt%) used in the tests above contains 0.076 mmol ($-SO_3H$). Based on this value, PTSA and RGO loading were determined for Test #5 and 6 in order to investigate the compounding effect of the two parts. As shown in Table 2, RGO had no detectable catalytic activity, PTSA itself showed certain catalytic activity, and the performance of (RGO+PTSA) mixture in Test #7 was similar to that of the pure PTSA. However, neither PTSA nor the mixture of (RGO+PTSA) was as good as SG, on

which not only was the conversion higher, but also the selectivity of (DTBGs+TTBG) significantly increased. These results manifests that there is a synergy on SG between the benzenesulfonic acid groups and the graphene substrate rather than a simple physical mixing. This is believed to be due to the amphiphilic property of SG with the grafted benzenesulfonic acid groups as its hydrophobic part and the graphene substrate as its hydrophilic section. Moreover, SG is quite light and can easily suspend in a liquid with suitable solvent affinity to achieve good dispersion. Since isobutene has very low solubility in glycerol, liquefied isobutene and glycerol initially stayed in two phases. An emulsion type of mixture formed with vigorous stirring. Amphiphilic SG might disperse along the phase interface and was accessible by both glycerol and isobutene, or it might stay in the glycerol but helped to attract isobutene to the glycerol. This is vital for both of the feeds, isobutene and glycerol, to access the catalyst simultaneously so as to react. Another typical characteristic of SG is that the oligomerization of isobutene on SG is minimal, just like on PTSA. Even with a $R_{IB/Gly}$ as high as 6, the mass fraction of DiB in the products (DiB wt%) from Test #4 was only 0.6 wt%. This is far lower than the values from most of the heterogeneous catalysts, such as Amberlyst-15, sulfonated zeolites and sulfonated peanut, etc., as listed in Table 1. Most of the grafted sulfonic acid groups on these catalysts are likely inside their pores which may result in diffusion limitation. Because graphene has an open structure, it is easy for reactants and the products to approach or leave the acid sites. This would eliminate prolonged residence time and thus avoid isobutene oligomerization/catalyst deactivation. The different deactivation behaviors may also come from the acidity difference. Although sulfonic acid groups are grafted, for example, the zeolites may still have some of their original acid groups, which could catalyze oligomerization of isobutene and cause deactivation.

Since there is negligible oligomerization of isobutene on the SG catalyst and unconverted isobutene can be recovered easily through gas/liquid separation, a high isobutene/glycerol ratio is practical to be used in order to drive the reaction to obtain high yield of the desired DTBGs and TTBG products. For solid catalysts containing benzenesulfonic groups, it can be deduced from structure characteristics point of view that the catalysts with three-dimension (3D) structures such as Amberlyst,[15,28] sulfonated zeolite[29] and sulfonated peanut shell catalyst[27] are prone to forming DiB, and the catalysts with open environment around acid sites like SG and sulfonated silica aerogel[28] produce minimal amount of DiB. Therefore, the great performance of SG is attributed to the suitable acidity offered by the grafted benzenesulfonic acid groups, the special dispersion property from its amphiphilicity and the open environment around the acid sites provided by the two dimensional sheet.

3.2.2 Reaction-extraction cycle process

Etherification of glycerol with isobutene is a process involving a transition from biphase to monophase. In the beginning, liquefied isobutene and glycerol stay in two phases and the two phases will gradually merge as the etherification proceeds and eventually form one phase.[21] In our study, a monophase that contained glycerol ethers, SG and trace amount of glycerol formed at the end of the reaction, as shown in Fig. 6 a. When certain amount of fresh glycerol was added to the mixture and the extraction procedure described above was conducted, SG was completely drawn to the bottom glycerol phase, leaving a transparent liquid at the top (Fig.6 b). Usually extraction refers to mass flux of liquid substances between two phases. However, the SG catalyst as a solid can be completely extracted by glycerol like a liquid substance. This special property of SG is attributed to the nature of graphene, a soft flat sheet of carbon just one atom thick and adjustable amphiphilic surface through changing surface functional groups.[36] So SG is a heterogeneous catalyst but has some characteristics of homogeneous catalyst because it can be dispersed evenly in a liquid and can be extracted by a liquid. Further analysis found that the major components of the top phase were DTBGs, TTBG and a small quantity of MTBGs, and the bottom phase contained glycerol, SG and a small amount of glycerol ethers. SG was successfully separated from the ether products into the bottom phase. Based on this finding, a repetitive reaction-extraction operation scheme was invented, as shown in Scheme 1.

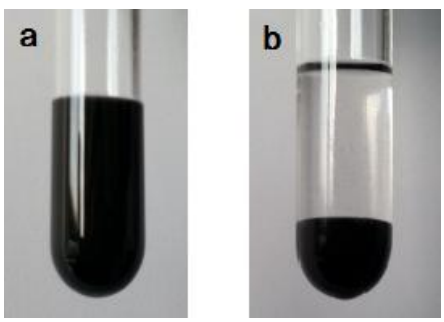

Fig. 6 Separation of reaction mixture with glycerol extraction: a. Mixture after reaction; b. After extraction with glycerol

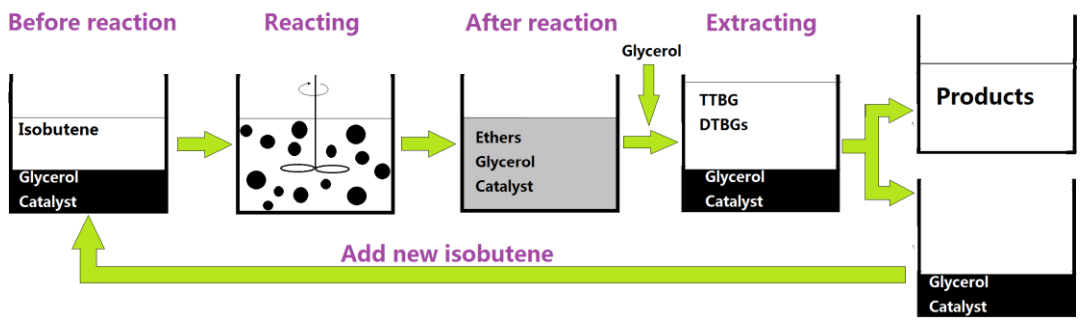

Scheme 1 Schematic diagram of reaction-extraction cycle process.

Table 3 Glycerol conversion, ether selectivitiy and top-phase product distribution for six reaction-extraction cycles.[a]

Reaction times	Conv.Gly. (mol%)	Selectivity (mol%)			Top-phase product distribution (wt%)			
		MTBGs	DTBGs	TTBG	MTBGs	DTBGs	TTBG	Others [b]
Cycle 1	99.1	4.4	52.2	43.4	1.5	45.9	51.0	1.0
Cycle 2	99.5	7.2	56.7	36.1	2.6	50.6	45.2	1.1
Cycle 3	99.8	5.9	57.6	36.5	3.0	51.9	43.5	0.9
Cycle 4	99.8	4.8	56.2	39.0	2.4	50.4	45.7	1.0
Cycle 5	99.6	5.6	55.7	38.8	2.3	49.9	46.2	1.2
Cycle 6	99.7	4.3	56.8	38.9	2.5	50.1	46.3	1.1

[a] $R_{cat/Gly}$ = 2 wt %; $R_{IB/Gly}$ = 6; 70 °C; 7h. [b] Others: IB and a few DiB and glycerol

Table 3 shows the results of six successive reaction-extraction cycles, including the glycerol conversion and ether selectivities after each reaction and the top-phase product distribution after each extraction. As indicated by the consistently high glycerol conversion throughout the six cycles, the catalyst showed no sign of deactivation. The selectivity of (DTBGs+TTBG) dipped slightly in Cycle 2 compared with Cycle 1, and then remained fairly stable afterwards. The majority of the top phase was DTBGs and TTBG (95 wt% or more), and the rest was MTBGs (1-3 wt%), IB (about 1 wt%) which could be easily removed by sparging with nitrogen or under negative pressure, a trace amount of DiB (0.1-0.3 wt%) and residual glycerol (no more than 0.2 wt%). The consistent performance during the repeated reaction-extraction cycles demonstrated that the catalyst was robust.

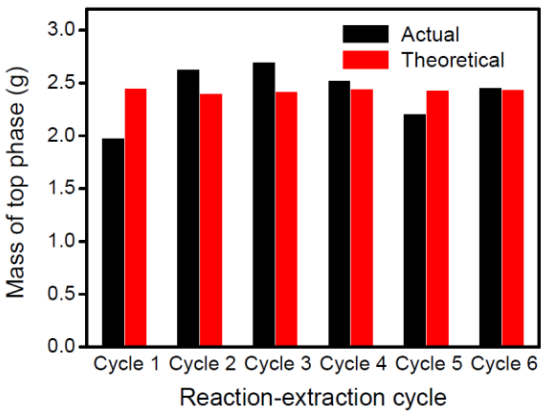

Fig. 7 Mass of the top phase after each extraction.

Fig. 7 shows the actual top phase product masses (black stripe) after each extraction and the corresponding theoretical values (red stripe), which was calculated from the product distribution after reaction, assuming all DTBGs and TTBG were the theoretical products and extracted to the top phase. The actual values of the products fluctuated around the theoretical ones due to variation from operation, but the average value (2.41 g) of the six actual mass numbers was nearly identical to that of the theoretical ones (2.33 g). During the six cycles, the total mass of collected top phase is 14.46 g, about 99 wt% of which is ethers; the mass of the ethers in the bottom phase of Cycle 6 is 0.14 g. Therefore, the total mass of ethers is 14.46 g. Since 6 g glycerol was added to react, the mass of ethers would be 14.60 g if we assume Cycles 2 to 6 have the same conversion and product distribution as Cycle 1. This is more like repeating Cycle 1 six times independently and collecting all the ether products. The actual mass of ethers is about 99% of the calculated value (14.46/14.60*100%), indicating the stable catalytic performance through the six cycles. From another aspect, the total product of the six consecutive cycles contains no less than 96.0 wt% di- and tri- butyl glycerol ethers, which is very close to the value of cycle 1, 96.9 wt%. All these results confirm the stabilities of the reaction-extraction process as well as the SG catalyst.

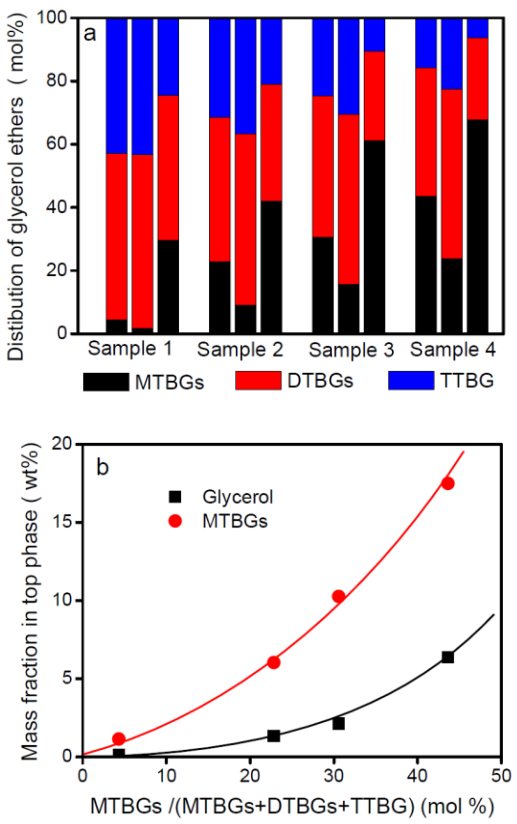

Fig. 8 Extraction performances of the samples with different original ether distributions: a. Distribution of MTBGs, DTBGs and TTBG of the samples: left, before extraction; middle, top phase after extraction; right, bottom phase after extraction; b. Glycerol and MTBGs in the top phase as a function of the proportion of MTBGs in glycerol ethers before extraction.

Our effort on the reaction-extraction process is to maximize the contents of di- and tri- butyl glycerol ethers and to minimize the contents of both glycerol and MTBGs in the top phase as much as possible. In order to find out the key factors that determine the final product composition, four samples with different original ether distributions collected from runs with different catalyst loadings or reaction time were used to demonstrate the component distribution before and after extraction. For each

sample in Fig. 8a, the three bars represent the relative contents of the ethers in the mixture before extraction, the top phase and the bottom phase after the extraction, respectively. Because they have stronger polarity than DTBGs and TTBG, MTBGs are prone to dissolve in glycerol. Therefore, it was not surprising to see that for all the four samples the extraction with glycerol selectively draw certain amount of MTBGs to the bottom phase and thus enriched DTBGs and TTBG in the top phase. With Sample 2, for example, the concentration of DTBGs and TTBG was increased from about 77 mol% in the product to about 91 mol% in the top phase. For the extraction, the ideal scenario is to have only di- and tri- butyl glycerol ethers in the top phase and both glycerol and MTBGs in the bottom phase. However, the amounts of glycerol and MTBGs in the top phase strongly depended on the proportion of MTBGs in glycerol ethers before extraction. As shown in the Fig. 8b, the more MTBGs in the ethers formed, the more MTBGs and glycerol the top phase would contain. This also means that the extraction efficacy could be limited. Diminishing the formation of MTBGs to minimal level during a reaction is vital to the success of the extraction. Due to the good catalytic performance of SG, the small amount of MTBGs in the product successfully suppressed the contents of both MTBGs and glycerol in the top layer product.

3.2.3 Study of reaction conditions

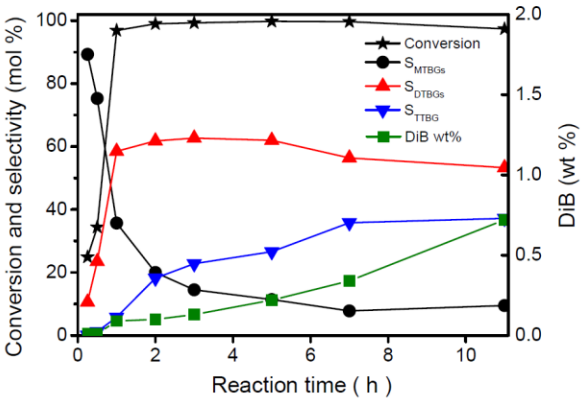

Fig. 9 Etherification of glycerol with isobutene at different reaction time ($R_{IB/Gly}$, 4 mol/mol; $R_{cat/Gly}$ = 4 wt%; 70 °C).

Fig. 9 summarizes the results obtained at different reaction time. The reaction was rapid, and the glycerol was almost completely consumed after 1 h. However, this did not mean the reaction was over. The fluctuations of the ethers' contents during the following period indicated that the etherification reaction was still continuing. The glycerol etherification is a tandem reaction that consists of three steps, among which the formation of DTBGs and TTBG is more time consuming. As shown by the selectivity plots in Fig. 9, the total selectivity to (DTBGs+TTBG) did not reach its maximum until 7 h, and after that the reaction seemed to reach an equilibrium since both the conversion of glycerol and the selectivities of ethers barely changed. Formation of multi-butyl glycerol ethers may also be sterically hindered on heterogeneous catalysts due to their relatively bulky size. But it seemed not to be an issue on SG due to its two-dimensional open structure. Another important aspect to consider is the isobutene oligomerization. It has been reported that the oligomerization of isobutene was irreversible.[11] Therefore, this side reaction should be minimized as much as possible. As can be seen in Fig. 9, DiB concentration increased gradually with increasing reaction time, but the issue of this side reaction was not serious on SG at all. The DiB formed was only 0.7 wt % even after 11 h reaction. .

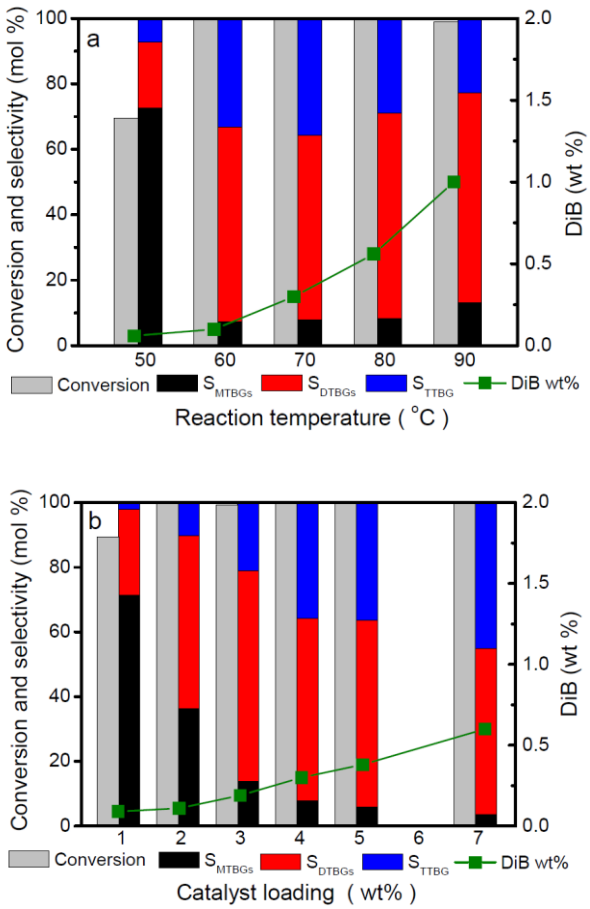

Fig. 10 Influence of reaction temperature and catalyst loading on glycerol etherification: a. at different reaction temperatures ($R_{IB/Gly}$, 4 mol/mol; $R_{cat/Gly}$ = 4 wt%; 7 h); b. at different catalyst loadings ($R_{IB/Gly}$, 4 mol/mol; 70 °C; 7 h).

Fig. 10a showed the effect of the reaction temperature. The conversion of glycerol at 50 °C was only 69.6%, and it quickly approached 100% when the reaction was conducted at 60 °C, above which the conversion stayed around 100%. The low reactivity at 50 °C may be because of poor mass transfer, since the viscosity of glycerol is very high at low temperature. With the temperature rising in the range of 50 to 90 °C, the total selectivity toward (DTBGs+TTBG) exhibited a volcano trend with a maximal value (more than 90 mol%) achieved around 60-70 °C, and the selectivity to MTBGs showed an opposite tendency. Because glycerol etherification with isobutene is a reversible and moderately exothermic reaction, higher reaction temperature favours the reverse reaction, which leads to increase in the dealkylation of the glycerol ethers, lowering the selectivity to (DTBGs+TTBG).[23] Increasing reaction temperature also aggravates the undesired dimerization of isobutene. As shown in Fig. 10a, DiB formation at 60-70 °C was below 0.3 wt%, and it

increased to 1.0 wt% when the temperature rose to 90 °C. With all these considered, 60-70 °C is considered the optimal range for the etherification on the catalyst.

Studies of catalyst loadings (Fig.10b) showed that nearly 90% glycerol was consumed under the reaction condition even when the catalyst loading was only 1 wt%, but MTBGs were the main product. Higher catalyst loading was needed to obtain more DTBGS and TTBG. As shown in Fig. 10b, the selectivity to MTBGs markedly decreased and the selectivity to DTBGs and TTBG changed in the opposite direction with increasing catalyst loading from 1 wt% to 7 wt%. Similar to long reaction time and/or high temperature, high catalyst loading also promoted the dimerization of isobutene. DiB yield increased from 0.1 wt% to 0.5 wt% when the catalyst loading increased from 1 wt% to 7 wt%. The gains on glycerol conversion and the selectivity of DTBGS and TTBG were not significant when the loading was above 4 wt%. Therefore, no more than 4 wt% loading was preferred at 70 °C.

4 Conclusion

Sulfonated graphene catalyst (SG) synthesized by grafting sulfonic acid groups to the two-dimensional surface of graphene was successfully applied to catalyze the etherification of glycerol with isobutene. Measure by glycerol conversion, multi-butyl ethers selectivity as well as DiB formation, the catalyst showed the best performance compared to those reported in the literature. At 60-70 °C with 4 wt% catalyst loading and a molar ratio of isobutene/glycerol 4, nearly a complete conversion of glycerol in 7 h and a selectivity of more than 92 mol% to desired multi-butyl glycerol ethers were achieved on the SG catalyst. Moreover, the undesired DiB was largely suppressed to 0.3 wt% or lower. The mixture after reaction was successfully layered to two phases with fresh glycerol addition. The top phase was a transparent product consisted of no less than 96 wt% di- and tri- butyl glycerol ethers, and the bottom phase was a black mixture containing glycerol, MTBGs, and SG, which was ready to start a new run with fresh isobutene addition. The catalyst presented robust performance in six consecutive reaction-extraction cycles. The great catalytic performance and the highly viable recycle process were largely attributed to the special properties of the SG catalyst, such as ultra thin two-dimensional open substrate, selective and stable sulfonated acid sites, amphiphilic property, and light texture. It is believed that this process with SG has high potential for practical practice.

Acknowledgement

The authors are grateful to the National Natural Science Foundation of China (Grant 21173027, Grant 21203015) and the Department of Education of Liaoning Province, China (Grant L2010037) for their financial support. We also thank the State Key Laboratory of Fine Chemicals at Dalian University of Technology for supporting the catalyst characterization in this work under Grant KF1109.

References

1 J. F. Izquierdo, M. Montiel, I. Pale´s, P. R. Outo´n, M. Gala´n, L. Jutglar, M. Villarrubia, M. Izquierdo, M. P. Hermo and X. Ariza, *Renewable and Sustainable Energy Rev*., 2012, **16**, 6717–6724.
2 M. Pagliaro, R. Cirimina, H. Kimura, M. Rossi, C. Della Pina, *Angew. Chem. Int. Ed*., 2007, **46**, 4434–4440.
3 A. Behr, J. Eilting, K. Irawadi, J. Leschinski and F. Lindner, *Green Chem.*, 2008, **10**, 13–30
4 H. J. Liu, D. H. Liu, and J. J. Zhong, *Biotechnol. Progr*., 2003, **19**, 1615–1619.
5 H. R. Jin, H. Y. Fang and J. Zhug, *Biotechnol. Lett*., 2003, **25**, 311–314.
6 H. Djelal, A. Amrane, F. Lahrer and G. Martin, *Appl. Microbiol. Biotechnol.*, 2005, **69**, 341–349.
7 G. Chen and S. Yao, *BioMed. Research. International.*, 2013, **2013**, 1–7.
8 M. Gupta, N. Kumar, *Renewable and Sustainable Energy Rev.*, 2012, **16**, 4551–4556.
9 A. Behr, L. Obendorf, *Chem. Ing. Tech.*, 2001, **73**, 1463-1467.
10 T. S. Viinikainen, R. S. Karinen, A. O. Krause, in: G. Centi, R. A. van Santen (Eds.), Production, Wiley-VCH Verlag GmbH and Co. KgaA, Weinheim, 2007.
11 K. Klepacova, D. Mr avec, M. Bajus, *Appl. Catal. A: Gen.*, 2005, **294** , 141–147.
12 J. Liu, B. Yang, and C. Yi, *Ind. Eng. Chem. Res.*, 2013, **52**, 3742−3751.
13 J. A. Melero, G. Vicente, G. Morales, M. Paniagua, J. M. Moreno, R. Roldán, A. Ezquerro and C. Pérez, *Appl. Catal. A: Gen.*, 2008, **346**, 44–51.
14 H. J. Lee, D. Seung, I. N. Filimonov and H. Kim, *Korean J. Chem. Eng* , 2011, **28**, 756 –762.
15 H. J. Lee, D. Seung, K. S. Jung, H. Kim, I. N. Filimonov, *Appl. Catal. A: Gen.*, 2010, **390**, 235–244.
16 A. Behr and L. Obendorf, *Eng. Life Sci.*, 2002, **2**, 185-189.
17 X. Liao, S. Wang, X. Xiang, Y. Zhu, X. She, Y. Li, *Fuel Process. Technol.*, 2012, **96**, 74–79.
18 M. D. Serio, L. Casale, R. Tesser and E. Santacesaria, *Energy Fuels*, 2010, **24**, 4668–4672.
19 K. Klepácová, D. Mravec, A. Kaszonyi and M. Bajus, *Appl. Catal. A: Gen*., 2007, **328**, 1–13.
20 K. Klepácová, D. Mravec and M. Bajus, *Chem. Pap.* 2006, **60**, 224–230.
21 R.S. Karinen and A.O.I. Krause, *Appl. Catal. A: Gen.*, 2006, **306**, 128–133.
22 H.J. Lee, D. Seung, K.S. Jung, H. Kim and I.N. Filimonov, *Appl. Catal. A: Gen.*, 2010, **390**, 235–244.
23 L. Xiao, J. Mao, J. Zhou, X. Guo and S. Zhang, *Appl. Catal. A: Gen.*, 2011, **393**, 88 –95.
24 M.D. Gonzalez, Y. Cesteros, P. Salagre, *Appl. Catal. A: Gen.*, 2013, **450**, 178-188.
25 W. Zhao, C. Yi, B. Yang, J. Hu and X. Huang, *Fuel Process. Technol.*, 2013, **112**, 70–75.
26 J. Janaun and N. Ellis, *J. of Appl. Sci.*, 2010, **10**, 2633–2637.
27 W. Zhao, B. Yang, C. Yi, Z. Lei and J. Xu, *Ind. Eng. Chem. Res.*, 2010, **49**, 12399–12404.
28 M. D. Gonzalez, P. Salagre, E. Taboada, J. Llorca, E. Molins and Y. Cesteros, *Appl. Catal., B*, 2013, **136–137**, 287–293.
29 M. D. González, P. Salagre, E. Taboada, J. Llorca and Y. Cesteros，*Green Chem.*, 2013, **15**, 2230–2239.
30 F. Frusteri, L. Frusteri, C. Cannilla and G. Bonura, *Bioresour.Technol*., 2012, **118**, 350–358.
31 A. K. Geim and K. S. Novoselov, *Natur. Mater.*, 2007, **6**, 183–191.
32 W.S. Hummers, R. E. Offeman, *J. Am. Chem. Soc.*, 1958, **80**, 1339–1339.
33 N. I. Kovtyukhova, P. J. Ollivier, B. R. Martin, T. E. Mallouk, S. A. Chizhik, E. V. Buzaneva and A. D. Gorchinskiy, *Chem. Mater.*, 1999, **11**, 771–778.
34 M. H. Rümmeli, C. G. Rocha, F. Ortmann, I. Ibrahim , H. Sevincli, F. Börrnert, J. Kunstmann, A. Bachmatiuk, M. Pötsche , M. Shiraishi, M. Meyyappan, B. Büchner, S. Roche and G. Cuniberti, *Adv. Mater.*, 2011, **23**, 4471–4490.

35 J. Ji, G. Zhang, H. Chen, S. Wang, G. Zhang, F. Zhang, X. Fan, *Chem. Sci.*, 2011, **2**, 484–487.
36 J. Kim, L.J. Cote, F.Kim, et al，Graphene Oxide Sheets at Interfaces，*J. Am. Chem. Soc*., 2010, **132**, 8180–8186.
37 C. N. R. Rao, A. K. Sood, K. S. Subrahmanyamm and A. Govindaraj, *Angew. Chem. Int. Ed.*, 2009, **48**, 7752–7777.
38 M. J. Allen, V. C. Tung and R. B. Kaner, *Chem. Rev*., 2010, **110**, 132–145.
39 Y. Zhu, S. Murali, W. Cai, X. Li, J. W. Suk, J. R. Potts, R. S. Ruoff, *Adv. Mater*., 2010, **22**, 3906-3924.
40 W.R. Collins, W. Lewandowski and E. Schmois, *Angew. Chem. Int. Ed*., 2011, **50**, 8848–8852.
41 T. M. G. Mohiuddin, A. Lombardo, R. R. Nair, A. Bonetti, G. Savini, R. Jalil, N. Bonini, D.M. Basko, C. Galiotis, N. Marzari, K.S. Novoselov, A.K. Geim and A.C. Ferrari, *Phys. Rev. B*, 2009, **79**, 205433–205440.
42 M. Jin, H. Jeong, T. Kim, K. P. So, Y. Cui, W.J. Yu, E.J. Ra and Y. H. Lee, *J. Phys. D: Appl. Phys.*, 2010, **43**, 275402–275402.
43 N. K Konstantin, O. Bulent, C. S. Hannes, K. P. Robert, A. A. Ilhan and C. Roberto, *Nano. Letters*, 2008, **8**, 36–41.